Article

pubs.acs.org/Biomac

Enhanced in Vitro Mineralization and in Vivo Osteogenesis of Composite Scaffolds through Controlled Surface Grafting of L-Lactic Acid Oligomer on Nanohydroxyapatite

Zongliang Wang,[†,¶] Yang Xu,[*,‡] Yu Wang,[†] Yoshihiro Ito,[§,⊥] Peibiao Zhang,[*,†] and Xuesi Chen[†]

[†]Key Laboratory of Polymer Ecomaterials, Changchun Institute of Applied Chemistry, Chinese Academy of Sciences, Changchun 130022, PR China

[‡]The First Hospital of Xiamen University, Xiamen 361003, PR China

[§]Nano Medical Engineering Laboratory and [⊥]Emergent Bioengineering Materials Research Team, RIKEN Center for Emergent Matter Science, RIKEN, 2-1 Hirosawa, Wako, Saitama 351-0198 Japan

[¶]University of Chinese Academy of Sciences, Beijing 100039, PR China

Supporting Information

ABSTRACT: Nanocomposite of hydroxyapatite (HA) surface grafted with L-lactic acid oligomer (LAc oligomer) (op-HA) showed improved interface compatibility, mechanical property, and biocompatibility in our previous study. In this paper, composite scaffolds of op-HA with controlled grafting different amounts of LAc oligomer (1.1, 5.2, and 9.1 wt %) were fabricated and implanted to repair rabbit radius defects. The dispersion of op-HA nanoparticles was more uniform than n-HA in chloroform and nanocomposites scaffold. Calcium and phosphorus exposure, in vitro biomineralization ability, and cell proliferation were much higher in the op-$HA_{1.1\ wt\ \%}$/PLGA scaffolds than the other groups. The osteodifferentiation and bone fusion in animal tests were significantly enhanced for op-$HA_{5.2\ wt\ \%}$/PLGA scaffolds. The results indicated that the grafted LAc oligomer of 5.2 or 9.1 wt %, which formed a barrier layer on the HA surface, prevented the exposure of nucleation sites. The shielded nucleation sites of op-HA particles (5.2 wt %) might be easily exposed as the grafted LAc oligomer was decomposed easily by enzyme systems in vivo. Findings from this study have revealed that grafting 1.1 wt % amount of LAc oligomer on hydroxyapatite could improve in vitro mineralization, and 5.2 wt % could promote in vivo osteogenesis capacity of composite scaffolds.

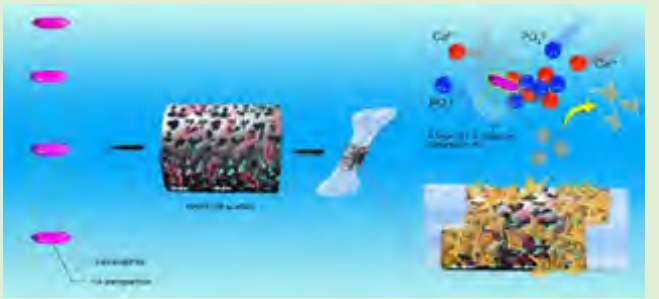

INTRODUCTION

Bone tissue engineering is mainly related to developing novel biomaterials as bone substitutes and grafts for treatment of bone defects, especially large bone loss.[1] Hydroxyapatite (HA), $Ca_2(PO_4)_6(OH)_2$, is a promising biomaterial used as bone substitute because it is a normal constituent of bone. HA has the particular ability to bind directly to bone without forming any surrounding connective tissue.[2] However, the major limitations to use HA ceramic are mechanical properties because it is brittle with a poor fatigue resistance.[3] In recent years, increasing attention has been focused on the development of HA composites. The combination of HA and biodegradable polymers is expected to overcome poor mechanical properties of HA ceramics.[4,5]

The composites of HA/Poly(lactic acid) (PLA) have been developed into orthopedical materials and medical products such as screws, plates, pins, and rods.[6] PLA is a biocompatible and biodegradable polyester belonging to the group of poly α-hydroxyacids. Compared with PLA, Poly(lactide-*co*-glycolide) (PLGA), the copolymer of lactide (LA) and glycolide (GA), is attracting more attention for tissue engineering application as its degradation can be easily manipulated by controlling the copolymer molecular weight and the LA/GA ratio. For this composite, the interaction and adhesion between HA filler and PLA (or PLGA) matrix are critical factors in determining the mechanical properties of the composite because lacking of adhesion between the two phases will result in an early failure at the interface and deteriorate the mechanical properties.

Various methods have been developed to improve the compatibility between the filler and the polymer such as silane coupling agents,[7] polyethylene glycol,[8] dodecyl alcohol,[9] zirconyl salts,[10] organicisocyanates,[11] and polyacids.[12] The coupling agent molecules were chemically reacted with the hydroxyl groups on the surface of HA, and the affinity of the particle surface to the polymer matrix was thus significantly improved. Biodegradable polymers such as poly(ε-caprolactone) (PCL),[13] poly(*N*-isopropylacrylamide) (PNIPAM),[14] and poly(L-lactide) (PLLA)[15−17] have also been used for

Received: November 14, 2015
Revised: January 12, 2016

DOI: 10.1021/acs.biomac.5b01543
Biomacromolecules XXXX, XXX, XXX−XXX

Scheme 1. (a) Synthesis of op-HA Surface Grafted with LAc Oligomer. (b) Schematic of n- and op-HA Nanoparticles with Different Grafting Ratio and Composite Scaffolds of n- and op-HA/PLGA for Bone Repair

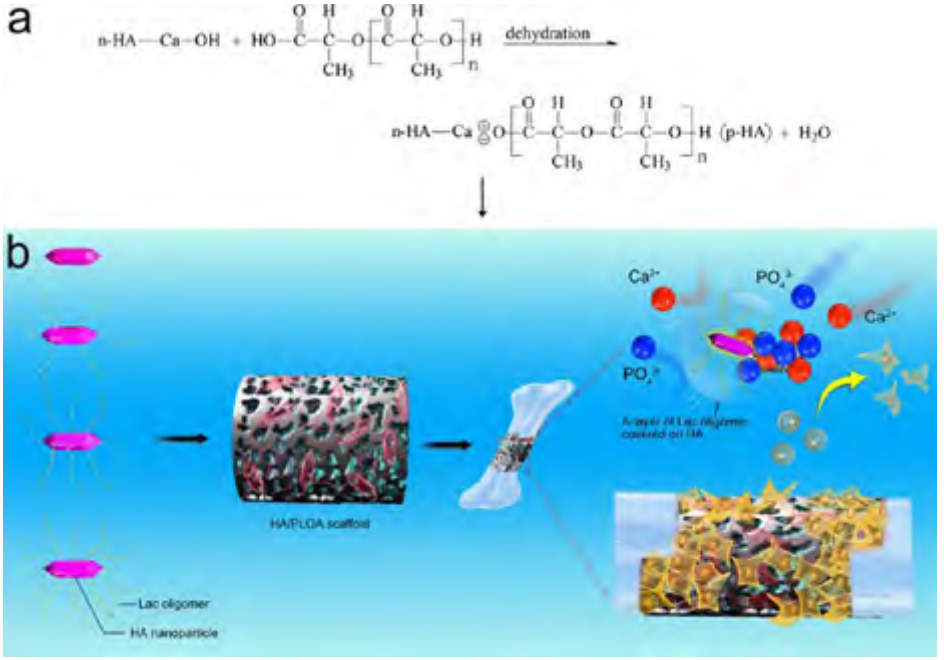

surface modification of HA. The amount of grafted polymer is a crucial factor for the property of the composites. It has been reported that 9.13 wt % combining stearic acid and L-lactide grafted on the HA particles improved more than 24.4% bending strength of the HA/PLGA composites[18] and 6 wt % poly(ε-caprolactone) (PCL) grafted improved 50% compressive strength of the HA/PCL composite scaffolds.[13] In our previous study, 6 wt % poly(L-lactic acid) (PLLA) grafted on the HA particle improved 20% tensile strength of the HA/PLLA composites.[19] Among these technologies, few studies pay attention to the influence of the grafting amount of coupling molecules on biomineralization and osteogenesis when their composite is applied as bone substitutes. It has been reported that biomaterials containing calcium phosphate (CaP) can promote osteogenic differentiation of progenitor and stem cells and can facilitate in vivo bone tissue formation.[20−22] Consequently, the grafted amount of coupling molecules on HA surface might obviously affect the Ca and P exposure and osteogenic differentiation in the composite scaffolds.

In our previous work, modification of hydroxyapatite nanoparticles by surface grafting reaction of L-lactic acid oligomer (LAc oligomer) (op-HA) in the absence of any catalyst and coupling agent has been developed.[23] The property of interface adhesion between op-HA and the polymer matrix and mechanical properties of the composite were significantly improved. In this study, as shown in Scheme 1, op-HA with controlled grafting different amounts of LAc oligomer was synthesized, and the composite scaffolds of op-HA/PLGA were prepared for investigating in vitro mineral deposition and in vivo osteogenesis ability.

EXPERIMENTAL SECTION

Materials. L-Lactide (LA) and glycolide (GA) were purchased from Purac, Holland. Stannous octoate ($Sn(Oct)_2$) was obtained from Sigma. Toluene, ethyl ether, chloroform, and ethanol were used as received. All chemicals were of analytical grade or higher.

Synthesis of Polymer and n-HA. Poly(lactide-*co*-glycolide) (PLGA, LA/GA = 80:20) with the viscosity's average molecular weight of 86 000, was synthesized in our lab by the ring opening copolymerization of the L-lactide and glycolide in the presence of stannous octoate ($Sn(Oct)_2$) as a catalyst.[15]

Needle-like HA nanocrystals (n-HA) of 20−30 nm in diameter and 100−200 nm in length were hydrothermally synthesized according to the following reaction equation:

$$10Ca(OH)_2 + 6H_3PO_4 \rightarrow Ca_{10}(PO_4)_6(OH)_2 + 18H_2O$$

Surface Grafting of n-HA. Controlled surface grafting of LAc oligomer onto HA surface was undertaken by forming a Ca carboxylate bond in the absence of any catalyst according to our previous work.[23] Briefly, LAc oligomer with the viscosity's average molecular weight of 1500 was prepared by the condensation reaction of L-lactic acid. It was dissolved in toluene, and then n-HA was dispersed in the solution. The mixture was heated to 110 or 140 °C and maintained for 20 or 50 min, and the water formed by the reaction was removed by azeotropic dehydration with toluene.

As shown in Table S1, to obtain op-HA with different grafting ratios, the feeding ratios (w/w) of n-HA and LAc oligomer were 50:1, 50:3, and 50:50, respectively. The surface modified n-HA powders (op-HA) were obtained after the mixture was washed five times with chloroform to remove the ungrafted LAc oligomer and dried in a vacuum oven at 60 °C for 24 h to remove the residual solvent. The reaction equation is presented in Scheme 1, panel a.

Characterization of op-HA Powder. The amount of surface grafted LAc oligomer was determined using the thermogravimetry analysis (TGA, TA Instruments TGA 500, USA). It was performed in air from room temperature to 800 °C at a rate of 20 °C·min^{-1} and using 10 mg samples. Both n- and op-HA powders were measured for comparison. The grafting ratios were calculated with the weight loss percentage during heating.

Fourier transformation infrared spectroscopy (FT-IR) (Bio-Rad Win-IR spectrometer, UK) was employed to characterize the surface-grafted HA particles. Both n- and op-HA particles were used directly for IR measurement in potassium bromide (KBr) disks. To confirm the grafting reaction, a film of the LAc oligomer on the KBr crystal plate was also characterized by FT-IR.

The morphology and crystallite size of n- and op-HA particles were observed on a transmission electron microscopy (TEM, JEM-2010

DOI: 10.1021/acs.biomac.5b01543
Biomacromolecules XXXX, XXX, XXX−XXX

JEOL, Japan) at an accelerating voltage of 100 kV. HA/chloroform suspensions with a concentration of 0.1% (w/v) were prepared by ultrasonically dispersing the n- or op-HA powders into chloroform. The TEM samples were prepared by dripping a drop of suspensions onto carbon coated copper grids and evaporating the solvent completely at room temperature. The samples were prepared using similar method for 6 and 24 h dispersion experiments.

Preparation of Nanocomposite. With the assistance of magnetic stirring and ultrasonic treatment, the dried n- or op-HA powders with different grafting ratios (1.1, 5.2, and 9.1 wt %) were uniformly suspended in 20-fold (w/v) chloroform. Then the suspension was added into a 6% (w/v) PLGA/chloroform solution to achieve the n- or op-HA content of 20 wt % in the composites. The mixture was precipitated in an excess of ethanol, and the composite was dried in a vacuum oven at 40−50 °C for 24 h to remove the residual solvent.

Fabrication of Porous Scaffolds. The porous scaffolds were prepared according to our previous method.[24] Briefly, sodium chloride (NaCl) particulates of 100−450 μm in diameter were added into melted PLGA, n- or op-HA/PLGA and mixed in an internal mixer at 160 °C, 60 rpm for 5 min. The weight ratios of salt particulates to the composites were 4:1. The blends were then molded into 4 mm-thick sheets, respectively, under 10 MPa pressure at 160 °C for 5 min before finally cooling to room temperature. The salt particles were subsequently removed from the composites by leaching in distilled water for 1 week, and the water was changed every 12 h. The porous scaffolds were then obtained after being air-dried for 72 h. The samples used for the following experiments were sterilized with ethylene oxide and kept in the vacuum.

Environmental Scanning Electron Microscopy (ESEM) Observation. An environmental scanning electron microscope (ESEM, XL30 FEG, Philips) was used to observe the microstructure of porous scaffolds. The samples were frozen in liquidized N_2 and quickly broken off to obtain a random brittle-fractured surface. A layer of gold was sprayed uniformly over the fractured surface before observation. Then energy dispersive X-ray spectrometry (EDX) (XL-30W/TMP, Philips, Japan) was employed to analyze the elements of calcium (Ca) and phosphorus (P).

In Vitro Biomineralization Test. The biomineralization of different scaffolds was studied by immersing samples in simulated body fluid (SBF) according to the literature.[25,26] The porous scaffolds with bars of 7 mm × 7 mm × 5 mm were immersed in 25 mL of SBF at 37 °C waving horizontally at 30 rpm for 8 w. The SBF was refreshed every 2 d. The pH value of SBF was monitored with a pH meter (S20K, Mettler-Toledo, Switzerland) every 2 d before 1 week immersion and every 2 weeks after 1 week immersion. Three samples of each scaffold were taken out at 1, 4, and 8 weeks and rinsed for 3−5 times with distilled water to wipe off the soluble salts. These samples were vacuum-dried for 48 h. The weight of each sample before and after immersion was recorded for accuracy. Moreover, the surface mineral deposition was observed with ESEM, and the contents of both calcium and phosphor were analyzed using the inductively coupling plasma atom emission spectrum (ICP-AES) (Thermo Jarrell Ash, USA).[27] In brief, about 20 mg of each sample was taken and quantified precisely before the sample was digested completely with 10 mL of nitric acid, vaporized, and dissolved in distilled water at a total volume of 25 mL. The calcium or phosphor concentration of the solution was analyzed by ICP-AES. Finally, the calcium or phosphor content of the sample was calculated according to the obtained concentration. Three parallel samples of each scaffold at all the time intervals were analyzed.

Cell Culture. Cell experiments were performed by using mouse preosteoblast MC3T3-E1 cells purchased from Institute of Biochemistry and Cell Biology, Shanghai Institutes for Biological Sciences, Chinese Academy of Sciences. Cells were cultured with Dulbecco's modified Eagle's medium (DMEM, Gibco) supplemented with 10% FBS (Gibco), 10 mM HEPES (Sigma), 63 mg L^{-1} penicillin (Sigma) and 100 mg L^{-1} streptomycin (Sigma) in a humidified incubator at 37 °C and 5% CO_2. The medium was changed every 2 d. When they reached at 80% confluence, the cells were harvested for the following assessment.

Cell Proliferation. Cell proliferation of MC3T3-E1 in the porous scaffolds was assayed using 3-(4,5-dimethyl-2-thiazolyl)-2,5-diphenyl tetrazolium bromide (MTT) method.[24] Briefly, the porous scaffolds were placed in the 24-well tissue culture plates (Costar). Four replicates were used for each sample. MC3T3-E1 cells (2×10^4 cells in 100 μL of medium) were seeded on each sample followed with addition of 1 mL of medium 4 h later and then incubated at 37 °C and 5% CO_2 for 3, 7, and 14 d, respectively. The medium was changed every other day. Four hours before each culture interval, 100 μL of MTT (5 mg/mL in PBS) was added to each well, and the cells were incubated for an additional 4 h. Once completed, the medium was removed, and 750 μL of acidified isopropanol (2 mL of 0.04 N hydrochloric acid (HCl) in 100 mL of isopropanol) was added to each well to solubilize the converted dye. The solution (200 μL) in each well was mixed and transferred to a 96-well plate, and optical density was measured at 540 nm wavelength on a Full Wavelength Microplate Reader (Infinite M200, TECAN). The mean value of the four replicates for each sample was used as the final result.

Osteogenic Differentiation. The expression of several osteogenic genes, ALP (alkaline phosphatase), Col-I (collagen type I), OCN (osteocalcin), and OPN (osteopontin), was analyzed by real-time polymerase chain reaction (PCR). After the MC3T3-E1 cells were cultured on scaffolds for 7 and 14 d, the cells were digested, and total RNA was isolated. Then the cDNA was synthesized using a PrimeScriptTM RT reagent kit (Takara Bio, Japan) according to the manufacturer's instructions. Highly purified gene specific primers (listed in Table 1) were synthesized commercially (Sangon, Co., Ltd. Shanghai, China). Quantification of bone marker genes was tested using a Stratagene 3005P real-time PCR system. For quantitative real-time PCR, 10 μL of SYBR Premix Ex TaqTM, 6.8 μL of dH_2O, 0.4 μL of each forward and reverse primer, 0.4 μL of Rox, and 2.0 μL of cDNA template were used in a final reaction volume of 20 μL. The PCR amplification cycles included denaturation for 5 s at 95 °C, annealing, and extension for 34 s at 56 °C for 40 cycles. Data collection was enabled at 56 °C in each cycle. CT (threshold cycle) values were calculated using the Stratagene MxPro software v4.01 system. Each gene expression value was normalized to that of the housekeeping gene, glyceraldehyde-3-phosphate dehydrogenase (GAPDH). Results were reported as relative gene expression. All experiments were done in triplicate to obtain the average data.

Table 1. Primer Sequences for Real-Time Polymerase Chain Reaction (Real-Time PCR)

gene	primer sequences
ALP	Forward: TATCTGCCTTGCCTGTATCTGG
	Reverse: GCTTTGGGAATCTGTGCAGTC
Col-I	Forward: CCAACAAGCATGTCTGGTTAGGAG
	Reverse: GCAATGCTGTTCTTGCAGTGGTA
OCN	Forward: AAGCAGGAGGGCAATAAGGT
	Reverse: TTTGTAGGCGGTCTTCAAGC
OPN	Forward: TCAGGACAACAACGGAAAGGG
	Reverse: GGAACTTGCTTGACTATCGATCAC
GAPDH	Forward: AACTTTGGCATTGTGGAAGG
	Reverse: ACACATTGGGGGTAGGAACA

Animal Tests. Bilateral critically sized defects of New Zealand white rabbits with body weight of 2.0−2.5 kg were created in the radius by removing 20 mm of midshaft diaphyseal bone.[27] The porous scaffolds with bars of 20 mm × 4 mm × 2 mm were placed into the defects, and the pure defect without any material was set as blank control. The wounds were closed with silk threads in layers. After surgery, the rabbits were returned to their cages and allowed to move freely. All rabbits were injected daily with penicillin intramuscularly with a dose of 400 000 units each for 1 week. All the wounds healed gradually, and the rabbits remained active with no postsurgery complications. Animals were kept in the Institute of Experimental

DOI: 10.1021/acs.biomac.5b01543
Biomacromolecules XXXX, XXX, XXX−XXX

Animals of Jilin University, in accordance with the institutional guidelines for care and use of laboratory animals.

X-ray Examination. Digital radiographs (DRs) of each foreleg were taken on KODAK CR 400 plus Filmless Radiology System (USA) at 0, 4, and 12 weeks after surgery to follow the healing process at the resection sites, and points were allotted according to the Lane−Sandhu scoring system.[28] All the points were given by five independent examiners who were trained in the Lane−Sandhu system. The points were given according to the degree of bone formation, connections, and bone marrow recanalization. For fully formed bone formation, 4 points were given; likewise, no bone formation was given 0 points. Depending on the degree of connection, according to the clearance of the fracture line, 0, 2, and 4 points were given. When no fracture line was detected, it was given 4 points, while a clear fracture line was given 0 points. For bone marrow recanalization, according to the degree of recanalization, 0, 2, or 4 points were given as well. The Lane−Sandhu radiographic scoring system is explained in Table 2.

Table 2. Lane−Sandhu Radiographic Scoring System

Degree of Bone Formation	
no new born formed	0
the area of new bone accounts for 25% of the defect area	1
the area of new bone accounts for 50% of the defect area	2
the area of new bone accounts for 75% of the defect area	3
the area of new bone accounts for 100% of the defect area	4
Degree of Union	
fracture line is fully visible	0
fracture line is partially visible	2
fracture line is not visible	4
Degree of Medullary Cavity Remodeling	
no sign of remodeling	0
recanalization of medullary cavity	2
cortical bone structure forms after recanalization of medullary cavity	4

Statistical Analysis. All quantitative data were analyzed with Origin 8.0 (OriginLab Corporation, USA) and expressed as the mean ± standard deviation. Statistical comparisons were carried out using the analysis of variance (ANOVA one-way, Origin 8.0). A value of $p < 0.05$ was considered to be statistically significant.

RESULTS AND DISCUSSION

TGA and FT-IR Analysis. The amount of grafted LAc oligomer was determined by TGA. As shown in Figure S1A, the weight loss of n-HA was only 0.8%, which might result from the evaporation of absorbed water on nanoparticles. The weight losses of obtained op-HA particles were 1.9%, 6.0%, and 9.9%, respectively. The amounts of surface-grafted LAc oligomer on op-HA were calculated as follows:

$$M_{(op-HA)} = W_{(op-HA)} - W_{(n-HA)} = 1.9\% - 0.8\% = 1.1\%$$

$$M_{(op-HA)} = W_{(op-HA)} - W_{(n-HA)} = 6.0\% - 0.8\% = 5.2\%$$

$$M_{(op-HA)} = W_{(op\text{-}HA)} - W_{(n-HA)} = 9.9\% - 0.8\% = 9.1\%$$

The grafted op-HA showed appreciable weight loss attributing to the decomposition of the grafted LAc oligomer and was thus taken as the grafting ratios of 1.1%, 5.2%, and 9.1%, respectively.

The grafting reaction of LAc oligomer on n-HA surface was verified by the FT-IR spectra. As shown in Figure S1B, the absorption intensities of the IR peaks at 1760 cm^{-1} of the grafting products indicate the increased grafting ratios. As illustrated in our previous report,[24] the absorption that emerged at 1716 cm^{-1} in the spectrum of op-HA was attributed to the carbonyl groups vibration, implying the formation of calcium carboxylate on the surface of n-HA.

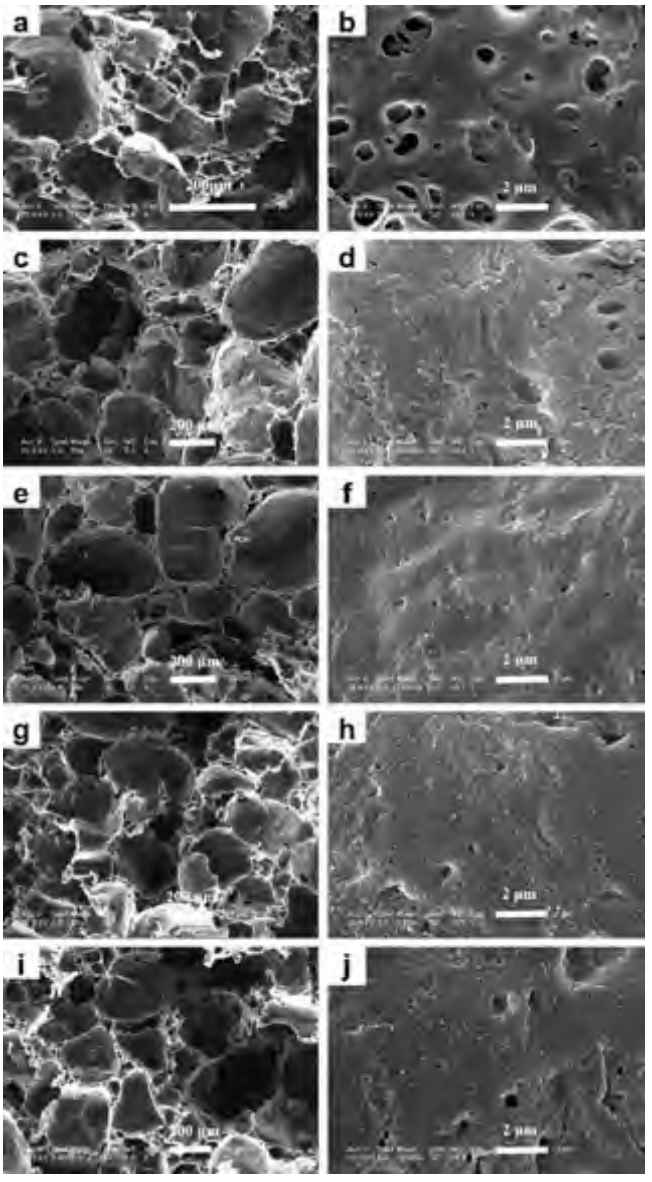

Figure 1. ESEM micrographs of (a, b) PLGA, (c, d) n-HA/PLGA, (e, f) op-$HA_{1.1\ wt\ \%}$/PLGA, (g, h) op-$HA_{5.2\ wt\ \%}$/PLGA, and (i, j) op-$HA_{9.1\ wt\ \%}$/PLGA porous scaffolds. The right images present the pore surface topography of those left images. Scale bar lengths are 200 μm (left images) and 2 μm (right images).

Influence of Grafting Ratios on Suspension Stability and Dispersion of Nanoparticle. As shown in Figure S2, the suspension stability of n-HA (or op-HA)/chloroform at different time intervals was observed. The n-HA nanoparticles precipitated in the organic solution immediately, but the op-HA exhibited excellent colloid stability and could maintain a stable dispersion in suspension for longer time even if the grafting ratio was only 1.1 wt %. Among the groups of op-HA, the visible precipitation appeared at 6 h in the group of 1.1 wt % op-HA and 24 h in the group of 5.2 wt % op-HA. Only 9.1 wt % op-HA kept its suspension stability for more than 24 h. The solution stability increased obviously with the rise of grafting ratios from 1.1 to 9.1 wt %. The results show that the surface modification of HA by the LAc oligomer could significantly

DOI: 10.1021/acs.biomac.5b01543
Biomacromolecules XXXX, XXX, XXX−XXX

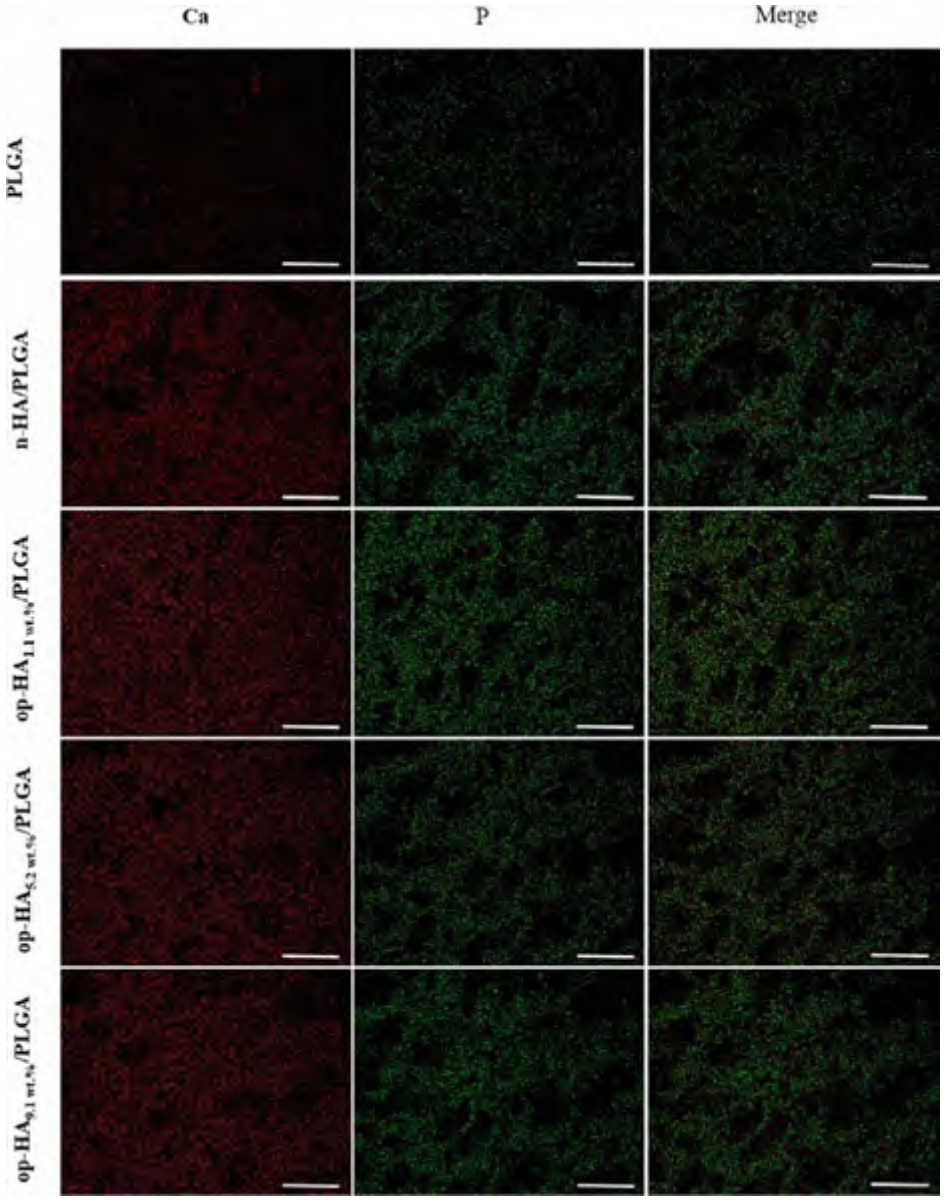

Figure 2. EDX maps of PLGA, n- and op-HA/PLGA porous scaffolds. Ca is red, and P is green. Bar lengths are 200 μm.

Table 3. Surface Elements of Different Scaffolds Analyzed with EDX

samples	C	O	P	Ca
n-HA/PLGA	36.73 ± 8.39	34.95 ± 5.94	10.40 ± 1.52	17.93 ± 2.83
op-$HA_{1.1\ wt\ \%}$/PLGA	21.82 ± 2.05	40.39 ± 4.31	12.04 ± 1.19	25.75 ± 5.15[a]
op-$HA_{5.2\ wt\ \%}$/PLGA	32.57 ± 6.22	35.55 ± 5.12	11.01 ± 2.85	20.87 ± 6.72
op-$HA_{9.1\ wt\ \%}$/PLGA	29.21 ± 4.16	42.10 ± 7.52	10.83 ± 1.90	17.86 ± 4.23

[a] $p < 0.05$, compared with n-HA/PLGA and op-$HA_{9.1\ wt\ \%}$/PLGA.

change its surface hydrophobic property and prevent nanoparticles from aggregation in organic solvent.

The dispersion of op-HA in chloroform was further verified with TEM observation. As shown in Figure S3, the n-HA was apt to accumulate together and formed larger aggregate. The dispersion of op-HA was improved greatly after the surface modification of the LAc oligomer, and more uniform dispersion was observed when the grafting ratio was increased from 1.1 to 9.1 wt %. This is in good accordance with the preliminary results concerning nanolevel dispersion of grafted HA particles in pure methylene chloride.[19,29] The results indicate that surface grafting of n-HA particles with a certain amount of LAc oligomer is an effective approach for preparing a homogeneous nanocomposite.

Microstructure and Surface Elements of Scaffolds. In our previous studies, the surface modification of n-HA with LAc oligomer can generate homogeneous rough surfaces in nanocomposite scaffolds.[24] The microscale or nanoscale surface roughness is regarded to be beneficial for cell adhesion, migration, and proliferation.[30]

As shown in Figure 1, the pores of all scaffolds were irregular and interconnected, and all the composite scaffolds (Figure

DOI: 10.1021/acs.biomac.5b01543
Biomacromolecules XXXX, XXX, XXX−XXX

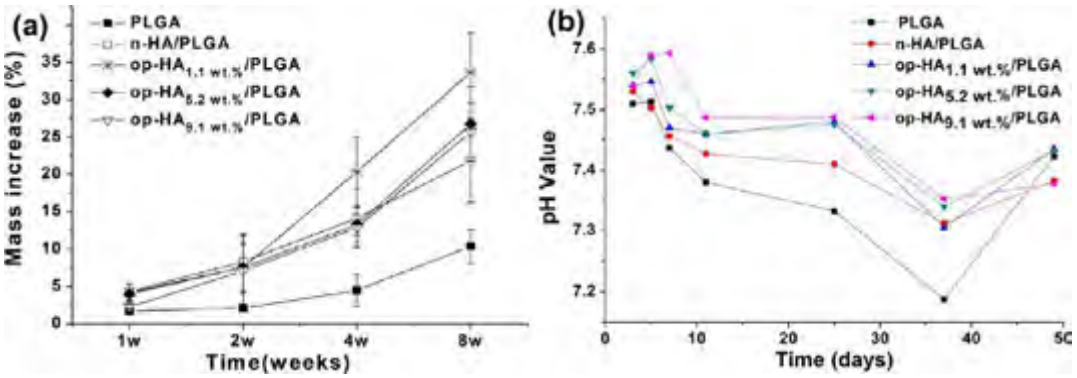

Figure 3. (a) Mass changes of different scaffolds immersed in SBF. (b) pH value changes of SBF as degradation of different scaffolds.

1c,e,g,i) presented relatively homogeneous pore structure compared to the PLGA scaffold (Figure 1a). The pore wall surfaces of the composite scaffolds (Figure 1d,f,h,j) were rougher than that of PLGA scaffold (Figure 1b). There were obvious differences in pore wall surfaces among the composite scaffolds with a large quantity of n-HA aggregates on the pore wall of n-HA/PLGA scaffold. While the distributions of op-HA on the pore wall of op-HA/PLGA scaffolds were more uniform, it was deduced that the grafted LAc oligomer improved the distribution of nanoparticles in the polymer matrix.

The surface element analyses of different scaffolds are shown in both Figure 2 and Table 3. As shown in Figure 2, EDX maps showed more Ca (red) and P (green) exposure on the surface of op-HA/PLGA scaffolds, especially for the op-$HA_{1.1\ wt\ \%}$/PLGA scaffold. The quantitative results showed that the Ca content of op-$HA_{1.1\ wt\ \%}$/PLGA was (25.75 ± 5.15)%, significantly higher than the others ($p < 0.05$). The Ca content of op-$HA_{5.2\ wt\ \%}$/PLGA was (20.87 ± 6.72)% and higher than that of op-$HA_{9.1\ wt\ \%}$/PLGA (17.86 ± 4.23%) and n-HA/PLGA (17.93 ± 2.83%) ($p > 0.05$). Similarly, the P content of all op-HA/PLGA was higher than that of n-HA/PLGA and decreased slightly with the increase of grafting ratios. However, there were no significant differences in P content among the composites. The results indicate that the Ca and P exposure of composite scaffolds is influenced by the surface modification of LAc oligomer and its grafting ratio to a certain extent. For n-HA/PLGA scaffold, the n-HA particles tend to aggregate and decrease the total exposure amount of n-HA on the pore wall of scaffold, while the op-HA particles are easily dispersed in polymer matrix, and more op-HA nanoparticles are exposed on the pore wall surface. Hence, more Ca and P exposure appears, and better biomineralization and osteogenic ability might be obtained.

In Vitro Biomineralization. Like other bioactive glasses and ceramics, HA is a time-dependent kinetic modification of the surface that occurs upon implantation.[3] The surface formed hydroxy carbonate apatite (HCA) layer is chemically and structurally equivalent to the mineral phase in bone and can provide the bonding interface with the bone tissues.[31] Thus, the test of in vitro biomineralization of a material is important in evaluating its in vivo osteogenic ability. In the present study, mass change, pH value of SBF, ESEM observation, and the ICP-AES detection of samples in SBF were employed for assaying their biomineralization.

Figure 3, panel a shows the mass changes of different scaffolds after immersing them in SBF for 1−8 weeks. All scaffolds showed a monotonic increase in mass within the immersion time. The rates of mass increase during this time were significantly lower for PLGA than for the composite scaffolds ($p < 0.05$), indicating the presence of n- or op-HA particles can accelerate the mass increase in the scaffolds. Among the first 2 weeks, the increased mass of n-HA/PLGA was slightly higher than that of op-HA/PLGA. After immersion for 4−8 weeks, op-$HA_{1.1\ wt\ \%}$/PLGA presented the highest rate of mass increase among all the scaffolds. Compared with n-HA/PLGA, the increased masses of op-$HA_{5.2\ wt\ \%}$/PLGA and op-$HA_{9.1\ wt\ \%}$/PLGA were still slightly lower at 4 weeks but became higher at 8 weeks.

The mass change of a scaffold in SBF is dedicated to its comprehensive effects including mineral deposition and material degradation. The degradation of composite scaffolds will result in the release of acid products and alkalescent ions. Thus, the pH changes of the SBF immersing different scaffolds were monitored as shown in Figure 3, panel b. At the initial stage (3−5 d after immersion), the pH value of PLGA was kept at about 7.51, and the pH value of n-HA/PLGA decreased minimally from 7.53 to 7.50. Only the composite scaffolds of op-HA/PLGA presented a slight increase of pH value, and the increased range was enlarged with the increase of grafting ratios. It may be associated with the release of alkalescent ions of op-HA on the surface of op-HA/PLGA scaffolds. Higher grafting ratio of op-HA led to higher density of op-HA exposed to the surface of composite scaffolds because of improved distribution of nanoparticles. After immersion for 7 d, the pH value of all samples began to decrease and reached its lowest point at 37 d. It indicated that PLGA began to degrade after 1 week of immersion and reached the fastest degradation rate at 5−6 weeks of immersion. During this stage, PLGA continuously presented the lowest pH value (pH = 7.18 at 37 d) because of its only existent polymer degradation products. The pH levels of n-HA/PLGA were between those of PLGA and op-HA/PLGA during the 7−37 d and were similar to that of op-$HA_{1.1\ wt\ \%}$/PLGA (pH = 7.30) at 37 d. The composite op-$HA_{9.1\ wt\ \%}$/PLGA exhibited the highest pH values during this stage, and it was only a little different from op-$HA_{5.2\ wt\ \%}$/PLGA at 37 d. It indicated that the composite scaffolds of both n-HA/PLGA and op-HA/PLGA released not only acid degradation products of PLGA, but also alkalescent ions of HA, and the amount of released acid products was higher than that of alkalescent ions during this stage.

However, the pH values of all samples rebounded due to more alkalescent ions releasing or less polymer degradation and ultimately increased up to about 7.40 at 7 weeks. It was deduced that the different pH changes of n-HA/PLGA and op-

DOI: 10.1021/acs.biomac.5b01543
Biomacromolecules XXXX, XXX, XXX−XXX

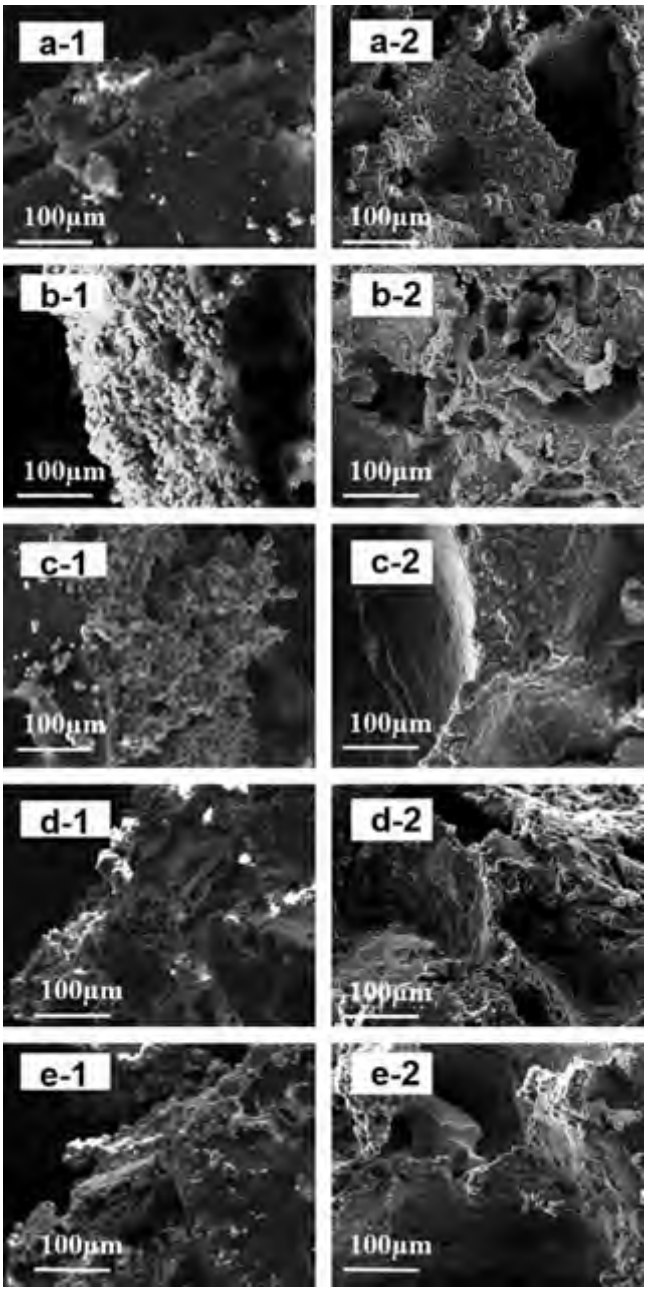

Figure 4. ESEM micrographs of (a) PLGA, (b) n-HA/PLGA, (c) op-$HA_{1.1\ wt\ \%}$/PLGA, (d) op-$HA_{5.2\ wt\ \%}$/PLGA, and (e) op-$HA_{9.1\ wt\ \%}$/PLGA scaffolds immersed in SBF for 4 weeks (−1) and 8 weeks (−2). Bar lengths are 100 μm.

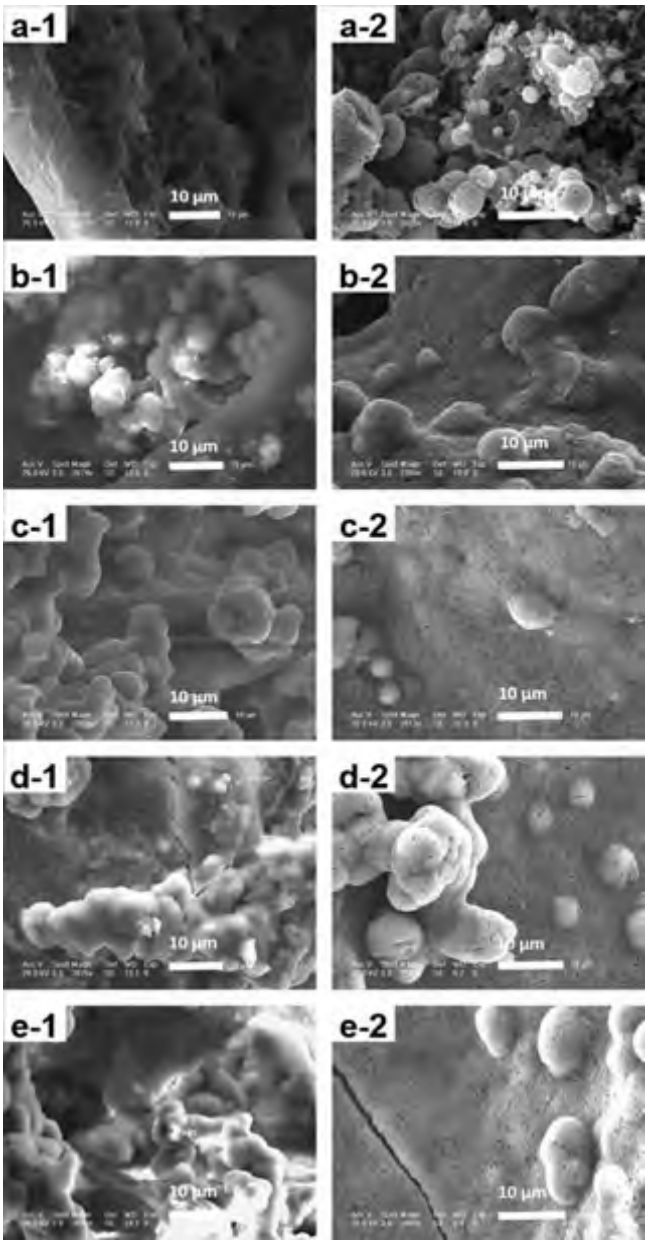

Figure 5. High-magnification ESEM micrographs of surface topography of (a) PLGA, (b) n-HA/PLGA, (c) op-$HA_{1.1\ wt\ \%}$/PLGA, (d) op-$HA_{5.2\ wt\ \%}$/PLGA, and (e) op-$HA_{9.1\ wt\ \%}$/PLGA scaffolds immersed in SBF for 4 weeks (−1) and 8 weeks (−2). All bar lengths are 10 μm.

HA/PLGA are related to the surface distribution of n- or op-HA nanoparticles in scaffolds. The present study also proves that the incorporation of n-HA in polymer scaffolds can help to maintain the microenvironment of the implant (such as pH values) so as to lighten the inflammation of implant degradation. The higher grafting ratio of Lac oligomer on n-HA will make a higher pH stability of microenvironment in a certain time.

As shown in Figures 4 and 5, the surface morphology of different porous scaffolds immersed in SBF for 4 and 8 weeks, respectively, was observed with ESEM under low- and high-magnification. After immersion for 4 weeks, there were only a few apatite particles deposited on the surface of PLGA scaffold (Figure 4a-1), while an apatite layer covered with a large quantity of micro particles was observed on the surfaces of the composite scaffolds (Figure 4b-1,c-1,d-1,e-1). Also, n-HA/PLGA (Figure 4b-1) and op-$HA_{1.1\ wt\ \%}$/PLGA (Figure 4c-1) composite scaffolds seemed to present more and larger areas of apatite particles than the others. According to high-magnification observation, the texture of PLGA scaffold became looser (Figure 5a-1). The apatite particles in composite scaffolds were about 3−5 μm in diameter and most of them fused together (Figure 5b-1,c-1,d-1,e-1). After immersion for 8 weeks, the PLGA scaffold also exhibited obvious mineralization, but its pore wall was thinner and more fragile (Figures 4a-2 and 5a-2) because of continuous degradation. Its surface was covered with a thin apatite layer consisting of a large quantity of microapatite particles (about 1−5 μm in diameter). Contrarily, all composite scaffolds were covered with a heavy apatite layer, and the pore

DOI: 10.1021/acs.biomac.5b01543
Biomacromolecules XXXX, XXX, XXX−XXX

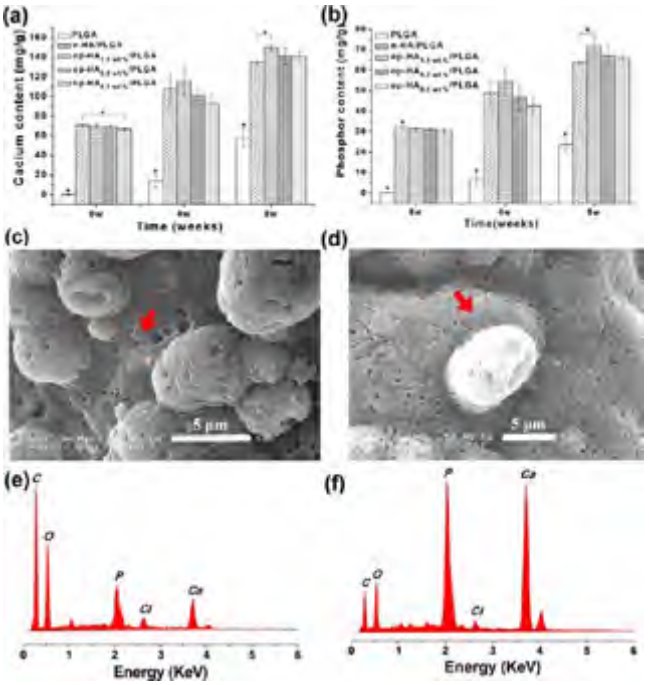

Figure 6. The contents of (a) Ca and (b) P in different scaffolds analyzed with ICP-OES. ∗, $p < 0.05$ compared with the other groups, $n = 3$. ESEM micrographs of (c) PLGA and (d) op-$HA_{1.1\ wt\ \%}$/PLGA scaffolds immersed in SBF for 8 weeks. The bars are 5 μm. EDX analysis of (e) PLGA and (f) op-$HA_{1.1\ wt\ \%}$/PLGA scaffolds at the area of red arrow indicated in panels c and d, respectively.

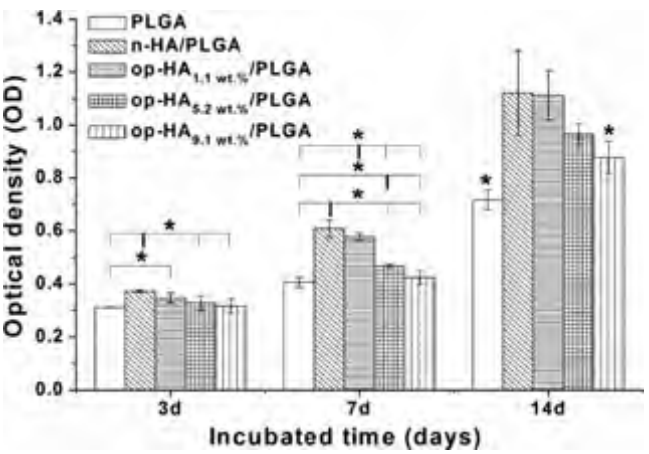

Figure 7. MC3T3-E1 cell proliferation in the different scaffolds. ∗, $p < 0.05$, $n = 4$.

walls became thicker and stiffer (Figure 4b-2,c-2,d-2,e-2). Only a few larger apatite particles (about 5−10 μm in diameter) could be observed from the apatite layers (Figure 5b-2,c-2,d-2,e-2). The distinct surface morphology at 8 weeks was a large quantity of worm-like etched pits emerged on the surface of the apatite layer or apatite particles, which was greatly different from those at 4 weeks. It was also very different from the literature.[32] Chen et al. reported that the typical "cauliflower" morphology of hydroxyapatite was formed on the surface of a 45S5 Bioglass-based foam (sintered at 1000 °C) after immersion in SBF for 28 days. However, no obvious differences in surface morphology and pore structure were observed in this study among the composite scaffolds with different grafting ratios of LAc oligomer.

The aforementioned results were verified further by ICP-AES analysis. As shown in Figure 6, panels a and b, the contents of Ca and P in all composite scaffolds were significantly higher than those of PLGA ($p < 0.05$) at all the time intervals. Before immersion, the Ca content of n-HA/PLGA (70.86 mg g^{-1}) was slightly higher than that of op-HA/PLGA (70.16 mg g^{-1}, 69.72 mg g^{-1}, and 67.13 mg g^{-1} for 1.1, 5.2, and 9.1 wt % op-HA/PLGA, respectively), and the difference in Ca content between n-HA/PLGA and op-$HA_{9.1\ wt\ \%}$/PLGA was significant ($p < 0.05$). After 4 and 8 weeks of immersion, the contents of Ca and P of all the samples increased greatly; especially op-$HA_{1.1\ wt\ \%}$/PLGA had the highest contents of Ca and P. Among the op-HA/PLGA scaffolds, the contents of Ca and P decreased obviously at 4 weeks and slightly at 8 weeks with the increase of grafting ratios. Compared with n-HA/PLGA, the contents of Ca and P in op-$HA_{5.2\ wt\ \%}$/PLGA and op-$HA_{9.1\ wt\ \%}$/PLGA decreased slightly at 4 weeks but still increased at 8 weeks. However, there were no significant differences among all composite scaffolds at either 4 or 8 weeks ($p > 0.05$). Nevertheless, the results of the ICP-AES analysis get along well with the mass change of scaffolds.

Figure 6, panels c and d showed that only a few mineralized particles appeared on the surface of PLGA scaffold, whereas a mineralization layer was formed on the surface of op-$HA_{1.1\ wt\ \%}$/PLGA scaffold. This could be proved by EDX results as the Ca and P were obviously detected from the composites either than PLGA (Figure 6e,f). The process of apatite formation on HA could be affected by bulk factors such as density and surface area as well as by surface factors such as composition and structure.[33] The results in this study suggested that a suitable grafting amount of LAc oligomer (1.1 wt %) on n-HA was favorable for mineral deposition because of its improved distribution of nanoparticles and more Ca and P exposure in the matrix. For higher grafting amount of LAc oligomer, the Ca and P exposure decreased as nanoparticles were enwrapped to some extent. In this study, PLGA scaffold also presented obvious mineral deposition, but its ability was significantly lower than the composite scaffolds. These findings indicate that appropriate grafting amount of LAc oligomer on the op-HA nanoparticles facilitates the formation of bone-like apatite on the polymer surface, which may increase the osteoinductive properties of this composite material and prove to be beneficial for its integration with living bone.[34]

Cell Proliferation. The challenge in developing biomaterials for engineered tissue is to create surfaces that can direct new tissue regeneration.[35] Also, the interaction of cells with surface topology has been proved to be a significant signaling modality in regulating cell functions such as cell adhesion, migration, and proliferation.[36] Figure 7 showed the cell proliferation of MC3T3-E1 cells grown on the different scaffolds. After 3 d of culture, the cell numbers of n-HA/PLGA and op-$HA_{1.1\ wt\ \%}$/PLGA were significantly higher than those of PLGA ($p < 0.05$). Compared with n-HA/PLGA, the cell number of op-HA/PLGA scaffolds decreased with raising of grafting ratios, and the differences were significant when grafting ratio was higher than 5.2 wt % ($p < 0.05$). However, there were no significant differences among the op-HA/PLGA scaffolds ($p > 0.05$). After 7 and 14 d of incubation, the cell number of all groups increased, and the differences among all the op-HA/PLGA scaffolds became enlarged. During the same time interval, the cell number of op-HA/PLGA scaffolds decreased with increase of grating ratios, especially when the grafting ratio was up to 9.1 wt % ($p < 0.05$). Only op-

DOI: 10.1021/acs.biomac.5b01543
Biomacromolecules XXXX, XXX, XXX−XXX

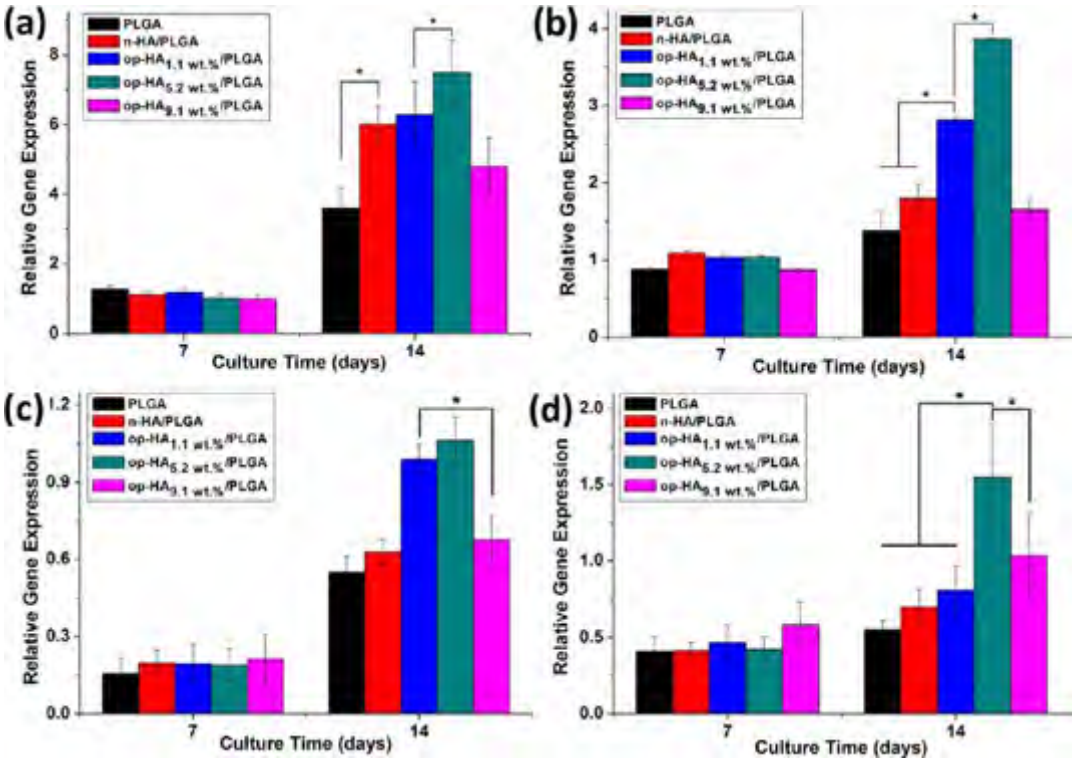

Figure 8. Expression of osteogenic genes including (a) ALP, (b) Col-I, (c) OCN, and (d) OPN by MC3T3-E1 cells grown in the different scaffolds for 7 and 14 d was analyzed by real-time PCR. The intensity of each gene was normalized to the value of GADPH. ∗, $p < 0.05$, $n = 3$.

$HA_{1.1\ wt\ \%}$/PLGA presented similar cell number compared to that of n-HA/PLGA. Nanoscaled surface topology has been shown to have positive effect on the cell behaviors.[37,38] The obtained results in this study indicated that the cell proliferation was improved by the nanoscaled topography of aggregated n-HA in the n-HA/PLGA scaffold and more Ca and P exposure in the op-$HA_{1.1\ wt\ \%}$/PLGA scaffold. The cell proliferation was affected obviously by the decreased Ca and P exposure due to nanoparticles enwrapped with LAc oligomer when grafting ratio was increased up to 9.1 wt %.

In Vitro Osteogenesis. Tissue engineering scaffolds with a highly porous structure can meet the needs of mass transfer of oxygen and nutrients for a large number of cells. Ca and P exposure of the pore wall surface is a key point for its biological activity. Because osteogenic differentiation of human marrow-derived cells can be prompted by PO_4^{3-} via affecting ATP synthesis,[20] and calcium is required for P-dependent ERK1/2 phosphorylation and regulation of mineralization-associated genes in osteoblasts,[21] we suppose that the difference in Ca and P exposure on the pore wall of scaffolds might affect their osteogenesis ability in vitro.

Therefore, the osteodifferentiation of MC3T3-E1 cells cultured on the scaffolds was also analyzed by the expression of several osteogenic genes via real-time PCR (Figure 8). After 7 d of culture, the expression of ALP did not show significant variations. The expression of Col-I was elevated to a higher level on the n-HA/PLGA, op-$HA_{1.1\ wt\ \%}$/PLGA, and op-$HA_{5.2\ wt\ \%}$/PLGA scaffolds compared with the others ($p > 0.05$). The expression of OCN was at a similar level on all the scaffolds, while the expression of OPN was a little higher on the op-$HA_{1.1\ wt\ \%}$/PLGA and op-$HA_{9.1\ wt\ \%}$/PLGA scaffolds ($p > 0.05$ vs the other groups). After 14 d of culture, all the studied genes were at a significantly higher level on op-$HA_{5.2\ wt\ \%}$/PLGA compared to the other groups ($p < 0.05$). Most interestingly, the expression of Col-I and OCN was significantly higher for both op-$HA_{1.1\ wt\ \%}$/PLGA and op-$HA_{5.2\ wt\ \%}$/PLGA than the other groups ($p < 0.05$). Also, the expression of ALP was significantly higher for n-HA/PLGA, op-$HA_{1.1\ wt\ \%}$/PLGA, and op-$HA_{5.2\ wt\ \%}$/PLGA than the other groups. The two main types of proteins in the extracellular matrix of bone are are collagens (mainly collagen type I) and the noncollagenous proteins, for example, osteocalcin (OCN).[39] OCN is known as the most specific protein for osteogenic matrix maturation and viewed as a marker for bone formation.[40] ALP is a well-established osteoblast phenotypic marker.[41] The real-time PCR results showed that bone-specific gene expression and mineralization of cells cultured in the op-$HA_{1.1\ wt\ \%}$/PLGA and op-$HA_{5.2\ wt\ \%}$/PLGA scaffolds were obviously enhanced compared to the other groups. It indicates that the op-$HA_{1.1\ wt\ \%}$/PLGA and op-$HA_{5.2\ wt\ \%}$/PLGA scaffolds can significantly enhance the osteodifferentiation of MC3T3-E1 cells.

Bone Healing. The radiographs of the rabbit radius defects implanted with porous scaffolds of PLGA, n-HA/PLGA, and op-HA/PLGA with different grafting ratios at 4 and 12 weeks postsurgery are shown in Figure 9. In this study, the bone defect of 20 mm in length in a bilateral rabbit radius was created. According to the literature,[42] it is the critical-sized model that the length of a bone defect is longer than that healing spontaneously.

At 4 weeks postsurgery, there was only a small bone callus formed at the end of the bone defect in the blank group (Figure 9a-2). However, the distinct bone callus emerged in the defect area that was replaced with the scaffolds (Figure 9b-2,c-2,d-2,e-2,f-2). The defects in the groups of the composite scaffolds of n-HA/PLGA, op-$HA_{1.1\ wt\ \%}$/PLGA, and op-$HA_{5.2\ wt\ \%}$/PLGA

DOI: 10.1021/acs.biomac.5b01543
Biomacromolecules XXXX, XXX, XXX−XXX

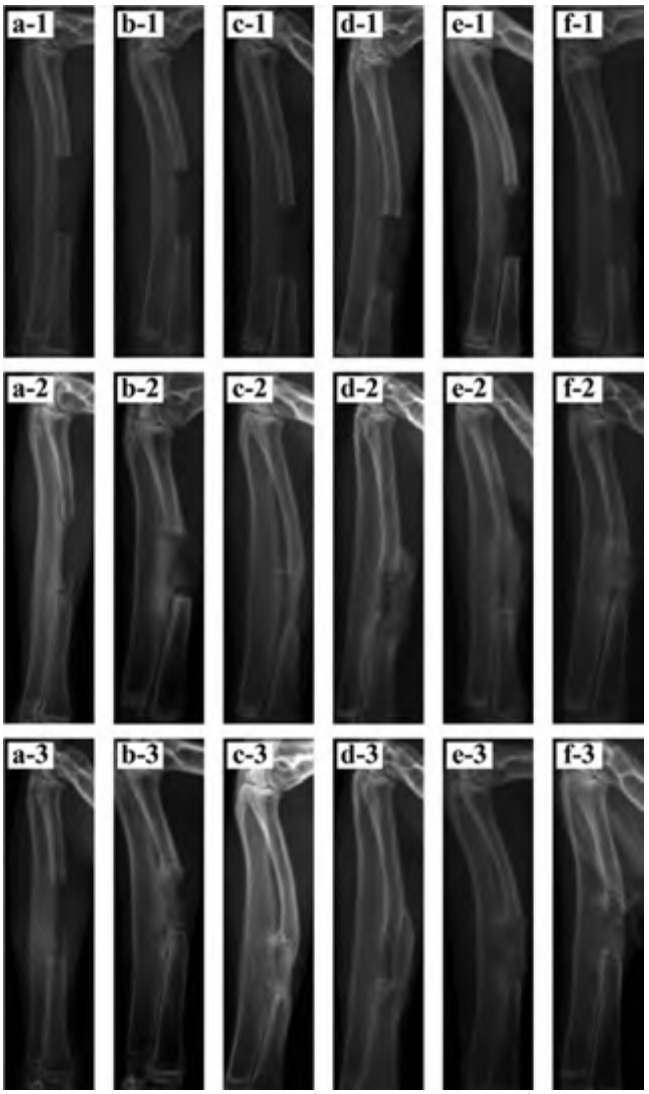

Figure 9. Digital radiographs of rabbit radius defects of (a) blank and implanted with (b) PLGA, (c) n-HA/PLGA, (d) op-$HA_{1.1\ wt\ \%}$/PLGA, (e) op-$HA_{5.2\ wt\ \%}$/PLGA, and (f) op-$HA_{9.1\ wt\ \%}$/PLGA scaffolds at 0 weeks (−1), 4 weeks (−2), and 12 weeks (−3).

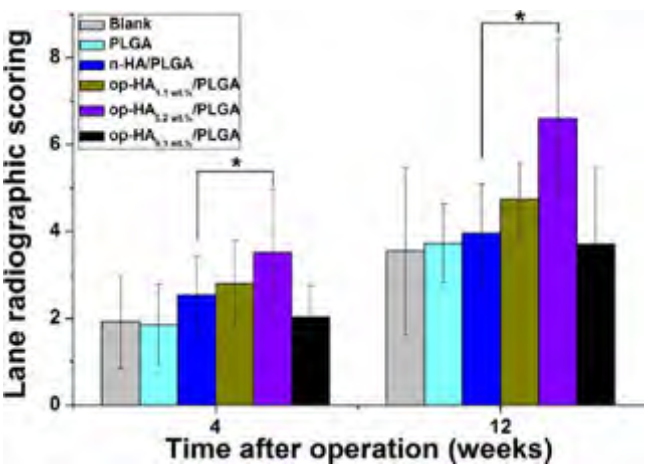

Figure 10. Lane−Sandhu radiographic scores of rabbit radius defects of blank control and implanted with different scaffolds at 4 and 12 weeks postsurgery. ∗, $p < 0.05$, $n = 3$.

were bridged with newly formed bones (Figure 9c-2,d-2,e-2). There was still a small gap between new bone in the group of PLGA or op-$HA_{9.1\ wt\ \%}$/PLGA, but the area of new bone in the group of op-$HA_{9.1\ wt\ \%}$/PLGA was larger than that of PLGA (Figure 9a-2,f-2). The group of n-HA/PLGA had the highest density of radiograph, and the group of op-$HA_{1.1\ wt\ \%}$/PLGA had the largest area of newly formed bone.

Meanwhile, at 12 weeks postsurgery, except for the blank group, all the defects implanted with the scaffolds were bridged, and the density of newly formed bone increased obviously. The groups of n-HA/PLGA, op-$HA_{1.1\ wt\ \%}$/PLGA, and op-$HA_{5.2\ wt\ \%}$/PLGA showed better bone fusion with the clear outlines of cortex and bone marrow cavities. Compared to the other groups, the area of the newly formed bone was less, and the density was lower in the group of PLGA. Although the defects in the group of op-$HA_{9.1\ wt\ \%}$/PLGA were bridged, the formed cortex was not clear and was considered non-continuous.

As shown in Figure 10, Lane−Sandhu scoring was performed on the bone defect sites of all the groups. The homogeneity test of variance was performed on Lane−Sandhu scores at all postoperative time points in the blank and experimental groups. There was a statistically significant difference among the scores obtained from op-$HA_{5.2\ wt\ \%}$/PLGA group compared to the other groups except for op-$HA_{1.1\ wt\ \%}$/PLGA at 4 weeks postsurgery ($p < 0.05$). The score obtained from op-$HA_{1.1\ wt\ \%}$/PLGA group was lower than that of op-$HA_{5.2\ wt\ \%}$/PLGA group without significant difference. The average score obtained from the op-$HA_{5.2\ wt\ \%}$/PLGA group was higher than the other groups with significant difference except for op-$HA_{1.1\ wt\ \%}$/PLGA at 12 weeks postsurgery ($p < 0.05$). The score obtained from op-$HA_{1.1\ wt\ \%}$/PLGA group was also lower than that of op-$HA_{5.2\ wt\ \%}$/PLGA group without significant difference. However, there was no statistically significant difference between the average score in the rest groups ($p > 0.05$).

The bone healing results were not well corroborated with the aforementioned results of element exposure, in vitro biomineralization, cell proliferation, and osteodifferentiation. The evenly distributed op-HA nanopartricles in PLGA matrix might provide more nucleation sites for apatite formation on the surface of pore wall. Unfortunately, with increasing grafting amounts of polymer onto the HA particles, the grafted LAc oligomer formed a barrier layer, and nucleation sites might be shielded (as shown in Scheme 1b). Therefore, the op-$HA_{1.1\ wt\ \%}$/PLGA scaffolds exhibited better mineral deposition and strong ability for in vitro biomineralization with more Ca and P exposure. However, the in vivo osteogenesis during fracture healing is a much more complex system with various enzymes affecting the bone repair process.[43,44] The findings of Einhorn[44] have shown that the chondrocytes release two types of enzymes-phosphatases and proteases to prepare the matrix for calcification during bone fracture healing process. The phosphatases provide phosphate ions to precipitate with the calcium delivered from the mitochondria and form calcified cartilage. The proteases degrade the proteoglycans that inhibit mineralization, allowing the chondrocytes to control the rate and physical chemistry of the mineralization process. Some recent investigations[45−48] found that the degradation of polylactic acid was obviously accelerated under different enzymes in vitro and in vivo. The shielded nucleation sites of op-$HA_{5.2\ wt\ \%}$/PLGA might be easily exposed as the grafted LAc oligomer was decomposed easily by enzyme systems in vivo.[49] Therefore, the in vivo osteogenesis of op-$HA_{5.2\ wt\ \%}$/PLGA

DOI: 10.1021/acs.biomac.5b01543
Biomacromolecules XXXX, XXX, XXX−XXX

scaffold was enhanced accompanied by the consequent biomineralization. These results implied that appropriate grafting amount of LAc oligomer and dispersibility of HA nanoparticles in polymeric matrix played an important role in definiting the osteogenesis ability.

CONCLUSIONS

Hydroxyapatite nanoparticles (n-HA) with surface controlled grafting different amount of L-lactic acid oligomer (LAc oligomer) (op-HA) were synthesized in the absence of any catalyst. The dispersion of op-HA nanoparticles was more uniform than n-HA in chloroform and nanocomposites. Calcium and phosphorus exposure, in vitro biomineralization ability, and cell proliferation were much higher in the op-$HA_{1.1\ wt\ \%}$/PLGA scaffolds than the others. The osteodifferentiation and bone fusion in vivo were significantly enhanced for op-$HA_{5.2\ wt\ \%}$/PLGA scaffolds. A barrier layer might be formed on the 5.2 or 9.1 wt % op-HA nanoparticles surface by the grafted LAc oligomer and prevented the exposure of nucleation sites. The shielded nucleation sites of op-HA particles (5.2 wt %) might be easily exposed as the grafted LAc oligomer was decomposed easily by enzyme systems in vivo. Findings from this study have revealed that grafting 1.1 wt % amount of LAc oligomer on hydroxyapatite could improve in vitro mineralization and 5.2 wt % could promote in vivo osteogenesis capacity of composite scaffolds. The results might promote the applications of op-HA/PLGA composites as bone regeneration substrates. More attention can be focused on the development of more active modified methods for HA nanoparticles, such as polypeptide or poly(amino acid), to improve the biological activity of composites scaffold.

ASSOCIATED CONTENT

Supporting Information

The Supporting Information is available free of charge on the ACS Publications website at DOI: 10.1021/acs.biomac.5b01543.

Dependence of grafting ratios on reaction condition, TGA and FT-IR profiles, dispersion of particles in chloroform, TEM micrographs of particles dispersed in chloroform (PDF)

AUTHOR INFORMATION

Corresponding Authors

*E-mail: zhangpb@ciac.ac.cn.

*E-mail: xuyang19792007@163.com.

Author Contributions

P.Z. and Y.X. designed the experiments. Z.W., Y.X., and Y.W. performed the experiments. Y.I. and X.C. supervised the research. Z.W. and P.Z. wrote the manuscript.

Notes

The authors declare no competing financial interest.

ACKNOWLEDGMENTS

This research was financially supported by National Natural Science Foundation of China (Projects. 51403197, 51473164, 51273195, and 51203152), the Ministry of Science and Technology of China (International Cooperation and Communication Program 2014DFG52510), the Joint funded program of Chinese Academy of Sciences and Japan Society for the Promotion of Science (GJHZ1519), and the Program of Scientific Development of Jilin Province (20130201005GX). Dr. Guoping Chen, National Institute for Materials Science, Japan, is appreciated for improving the English in this paper.

REFERENCES

(1) Shrivats, A. R.; McDermott, M. C.; Hollinger, J. O. Bone tissue engineering: state of the union. *Drug Discovery Today* **2014**, *19* (6), 781−786.

(2) Zhou, Q.; Xanthos, M. Nanoclay and crystallinity effects on the hydrolytic degradation of polylactides. *Polym. Degrad. Stab.* **2008**, *93* (8), 1450−1459.

(3) Dorozhkin, S. V. Bioceramics of calcium orthophosphates. *Biomaterials* **2010**, *31* (7), 1465−85.

(4) Li, D.; Guo, G.; Fan, R.; Liang, J.; Deng, X.; Luo, F.; Qian, Z. PLA/F68/dexamethasone implants prepared by hot-melt extrusion for controlled release of anti-inflammatory drug to implantable medical devices: I. Preparation, characterization and hydrolytic degradation study. *Int. J. Pharm.* **2013**, *441* (1−2), 365−72.

(5) Shi, Q.; Zhou, C.; Yue, Y.; Guo, W.; Wu, Y.; Wu, Q. Mechanical properties and in vitro degradation of electrospun bio-nanocomposite mats from PLA and cellulose nanocrystals. *Carbohydr. Polym.* **2012**, *90* (1), 301−8.

(6) Navarro, M.; Michiardi, A.; Castano, O.; Planell, J. A. Biomaterials in orthopaedics. *J. R. Soc., Interface* **2008**, *5* (27), 1137−1158.

(7) Borum, L.; Wilson, O. C. Surface modification of hydroxyapatite. Part II. Silica. *Biomaterials* **2003**, *24* (21), 3681−8.

(8) Liu, Q.; de Wijn, J. R.; de Groot, K.; van Blitterswijk, C. A. Surface modification of nano-apatite by grafting organic polymer. *Biomaterials* **1998**, *19* (11−12), 1067−72.

(9) Borum-Nicholas, L.; Wilson, O. C., Jr. Surface modification of hydroxyapatite. Part I. Dodecyl alcohol. *Biomaterials* **2003**, *24* (21), 3671−9.

(10) Misra, D. N. Adsorption of Zirconyl Salts and Their Acids on Hydroxyapatite - Use of the Salts as Coupling Agents to Dental Polymer Composites. *J. Dent. Res.* **1985**, *64* (12), 1405−1408.

(11) Liu, Q.; de Wijn, J. R.; van Blitterswijk, C. A. A study on the grafting reaction of isocyanates with hydroxyapatite particles. *J. Biomed. Mater. Res.* **1998**, *40* (3), 358−364.

(12) Liu, Q.; de Wijn, J. R.; Bakker, D.; van Toledo, M.; van Blitterswijk, C. A. Polyacids as bonding agents in hydroxyapatite polyester-ether (Polyactive (TM) 30/70) composites. *J. Mater. Sci.: Mater. Med.* **1998**, *9* (1), 23−30.

(13) Wang, Y.; Dai, J.; Zhang, Q. C.; Xiao, Y.; Lang, M. D. Improved mechanical properties of hydroxyapatite/poly(epsilon-caprolactone) scaffolds by surface modification of hydroxyapatite. *Appl. Surf. Sci.* **2010**, *256* (20), 6107−6112.

(14) Wei, J. C.; He, P.; Liu, A. X.; Chen, X. S.; Wang, X. H.; Jing, X. B. Surface Modification of Hydroxyapatite Nanoparticles with Thermal-Responsive PNIPAM by ATRP. *Macromol. Biosci.* **2009**, *9* (12), 1237−1246.

(15) Hong, Z. K.; Zhang, P. B.; Liu, A. X.; Chen, L.; Chen, X. S.; Jing, X. B. Composites of poly(lactide-co-glycolide) and the surface modified carbonated hydroxyapatite nanoparticles. *J. Biomed. Mater. Res., Part A* **2007**, *81A* (3), 515−522.

(16) Qiu, X. Y.; Hong, Z. K.; Hu, J. L.; Chen, L.; Chen, X. S.; Jing, X. B. Hydroxyapatite surface modified by L-lactic acid and its subsequent grafting polymerization of L-lactide. *Biomacromolecules* **2005**, *6* (3), 1193−1199.

(17) Bhuiyan, D.; Jablonsky, M. J.; Kolesov, I.; Middleton, J.; Wick, T. M.; Tannenbaum, R. Novel synthesis and characterization of a collagen-based biopolymer initiated by hydroxyapatite nanoparticles. *Acta Biomater.* **2015**, *15*, 181−190.

(18) Liuyun, J.; Xiong, C. D.; Chen, D. L.; Jiang, L. X.; Pang, X. B. Effect of n-HA with different surface-modified on the properties of n-HA/PLGA composite. *Appl. Surf. Sci.* **2012**, *259*, 72−78.

DOI: 10.1021/acs.biomac.5b01543
Biomacromolecules XXXX, XXX, XXX−XXX

(19) Hong, Z. K.; Qiu, X. Y.; Sun, J. R.; Deng, M. X.; Chen, X. S.; Jing, X. B. Grafting polymerization of L-lactide on the surface of hydroxyapatite nano-crystals. *Polymer* **2004**, *45* (19), 6699−6706.
(20) Shih, Y. R. V.; Hwang, Y.; Phadke, A.; Kang, H.; Hwang, N. S.; Caro, E. J.; Nguyen, S.; Siu, M.; Theodorakis, E. A.; Gianneschi, N. C.; Vecchio, K. S.; Chien, S.; Lee, O. K.; Varghese, S. Calcium phosphate-bearing matrices induce osteogenic differentiation of stem cells through adenosine signaling. *Proc. Natl. Acad. Sci. U. S. A.* **2014**, *111* (3), 990−995.
(21) Khoshniat, S.; Bourgine, A.; Julien, M.; Petit, M.; Pilet, P.; Rouillon, T.; Masson, M.; Gatius, M.; Weiss, P.; Guicheux, J.; Beck, L. Phosphate-dependent stimulation of MGP and OPN expression in osteoblasts via the ERK1/2 pathway is modulated by calcium. *Bone* **2011**, *48* (4), 894−902.
(22) Wen, L.; Wang, Y.; Wang, H.; Kong, L. M.; Zhang, L.; Chen, X.; Ding, Y. L-type calcium channels play a crucial role in the proliferation and osteogenic differentiation of bone marrow mesenchymal stem cells. *Biochem. Biophys. Res. Commun.* **2012**, *424* (3), 439−445.
(23) Qiu, X. Y.; Chen, L.; Hu, J. L.; Sun, J. R.; Hong, Z. K.; Liu, A. X.; Chen, X. S.; Jing, X. B. Surface-modified hydroxyapatite linked by L-lactic acid oligomer in the absence of catalyst. *J. Polym. Sci., Part A: Polym. Chem.* **2005**, *43* (21), 5177−5185.
(24) Cui, Y.; Liu, Y.; Cui, Y.; Jing, X. B.; Zhang, P. B. A.; Chen, X. S. The nanocomposite scaffold of poly(lactide-co-glycolide) and hydroxyapatite surface-grafted with L-lactic acid oligomer for bone repair. *Acta Biomater.* **2009**, *5* (7), 2680−2692.
(25) Kokubo, T.; Takadama, H. How useful is SBF in predicting in vivo bone bioactivity? *Biomaterials* **2006**, *27* (15), 2907−2915.
(26) Zhang, Q. W.; Mochalin, V. N.; Neitzel, I.; Hazeli, K.; Niu, J. J.; Kontsos, A.; Zhou, J. G.; Lelkes, P. I.; Gogotsi, Y. Mechanical properties and biomineralization of multifunctional nanodiamond-PLLA composites for bone tissue engineering. *Biomaterials* **2012**, *33* (20), 5067−5075.
(27) Zhang, P.; Hong, Z.; Yu, T.; Chen, X.; Jing, X. In vivo mineralization and osteogenesis of nanocomposite scaffold of poly(lactide-co-glycolide) and hydroxyapatite surface-grafted with poly(L-lactide). *Biomaterials* **2009**, *30* (1), 58−70.
(28) Lane, J. M.; Sandhu, H. S. Current Approaches to Experimental Bone-Grafting. *Orthop. Clin. North Am.* **1987**, *18* (2), 213−225.
(29) He, J. Q.; Yang, X. P.; Mao, J. F.; Xu, F. J.; Cai, Q. Hydroxyapatite-poly(L-lactide) nanohybrids via surface-initiated ATRP for improving bone-like apatite-formation abilities. *Appl. Surf. Sci.* **2012**, *258* (18), 6823−6830.
(30) Wang, G. C.; Liu, X. Y.; Zreiqat, H.; Ding, C. X. Enhanced effects of nano-scale topography on the bioactivity and osteoblast behaviors of micron rough ZrO2 coatings. *Colloids Surf., B* **2011**, *86* (2), 267−274.
(31) Rezwan, K.; Chen, Q. Z.; Blaker, J. J.; Boccaccini, A. R. Biodegradable and bioactive porous polymer/inorganic composite scaffolds for bone tissue engineering. *Biomaterials* **2006**, *27* (18), 3413−31.
(32) Chen, Q. Z.; Thompson, I. D.; Boccaccini, A. R. 45S5 Bioglass-derived glass-ceramic scaffolds for bone tissue engineering. *Biomaterials* **2006**, *27* (11), 2414−25.
(33) Kim, H. M.; Himeno, T.; Kokubo, T.; Nakamura, T. Process and kinetics of bonelike apatite formation on sintered hydroxyapatite in a simulated body fluid. *Biomaterials* **2005**, *26* (21), 4366−4373.
(34) Zhang, R. Y.; Ma, P. X. Porous poly(L-lactic acid)/apatite composites created by biomimetic process. *J. Biomed. Mater. Res.* **1999**, *45* (4), 285−293.
(35) Fan, X. X.; Ren, H. H.; Liu, P. Z.; Wang, P.; Li, H.; Yan, Y. G.; Lv, G. Y. Effects of the surface modification of poly(amino acid)/hydroxyapatite/calcium sulfate biocomposites on the adhesion and proliferation of osteoblast-like cells. *J. Appl. Polym. Sci.* **2015**, *132*, 33.
(36) Mao, H. L.; Kawazoe, N.; Chen, G. P. Cell response to single-walled carbon nanotubes in hybrid porous collagen sponges. *Colloids Surf., B* **2015**, *126*, 63−69.
(37) Solanki, A.; Chueng, S. T. D.; Yin, P. T.; Kappera, R.; Chhowalla, M.; Lee, K. B. Axonal Alignment and Enhanced Neuronal Differentiation of Neural Stem Cells on Graphene-Nanoparticle Hybrid Structures. *Adv. Mater.* **2013**, *25* (38), 5477−5482.
(38) Chen, Y. S.; Hsiue, G. H. Directing neural differentiation of mesenchymal stem cells by carboxylated multiwalled carbon nanotubes. *Biomaterials* **2013**, *34* (21), 4936−4944.
(39) Strobel, L. A.; Hild, N.; Mohn, D.; Stark, W. J.; Hoppe, A.; Gbureck, U.; Horch, R. E.; Kneser, U.; Boccaccini, A. R. Novel strontium-doped bioactive glass nanoparticles enhance proliferation and osteogenic differentiation of human bone marrow stromal cells. *J. Nanopart. Res.* **2013**, *15* (7), 1780.
(40) Hoang, Q. Q.; Sicheri, F.; Howard, A. J.; Yang, D. S. C. Bone recognition mechanism of porcine osteocalcin from crystal structure. *Nature* **2003**, *425* (6961), 977−980.
(41) Ducy, P.; Zhang, R.; Geoffroy, V.; Ridall, A. L.; Karsenty, G. Osf2/Cbfa1: A transcriptional activator of osteoblast differentiation. *Cell* **1997**, *89* (5), 747−754.
(42) Mokbel, N.; Bou Serhal, C.; Matni, G.; Naaman, N. Healing patterns of critical size bony defects in rat following bone graft. *Oral Maxillofac Surg* **2008**, *12* (2), 73−8.
(43) Wozney, J. M.; Rosen, V.; Celeste, A. J.; Mitsock, L. M.; Whitters, M. J.; Kriz, R. W.; Hewick, R. M.; Wang, E. A. Novel Regulators of Bone-Formation - Molecular Clones and Activities. *Science* **1988**, *242* (4885), 1528−1534.
(44) Einhorn, T. A. The science of fracture healing. *J. Orthop Trauma* **2005**, *19* (10), S4−S6.
(45) Lee, S. H.; Kim, I. Y.; Song, W. S. Biodegradation of polylactic acid (PLA) fibers using different enzymes. *Macromol. Res.* **2014**, *22* (6), 657−663.
(46) Song, Z. M.; Shi, B.; Ding, J. X.; Zhuang, X. L.; Zhang, X. N.; Fu, C. F.; Chen, X. S. A comparative study of preventing postoperative tendon adhesion using electrospun polyester membranes with different degradation kinetics. *Sci. China: Chem.* **2015**, *58* (7), 1159−1168.
(47) Ishii, D.; Ying, T. H.; Mahara, A.; Murakami, S.; Yamaoka, T.; Lee, W. K.; Iwata, T. In Vivo Tissue Response and Degradation Behavior of PLLA and Stereocomplexed PLA Nanofibers. *Biomacromolecules* **2009**, *10* (2), 237−242.
(48) Luzi, F.; Fortunati, E.; Puglia, D.; Petrucci, R.; Kenny, J. M.; Torre, L. Study of disintegrability in compost and enzymatic degradation of PLA and PLA nanocomposites reinforced with cellulose nanocrystals extracted from Posidonia Oceanica. *Polym. Degrad. Stab.* **2015**, *121*, 105−115.
(49) Malwela, T.; Ray, S. S. Enzymatic degradation behavior of nanoclay reinforced biodegradable PLA/PBSA blend composites. *Int. J. Biol. Macromol.* **2015**, *77*, 131−142.

DOI: 10.1021/acs.biomac.5b01543
Biomacromolecules XXXX, XXX, XXX−XXX